

Solvation and Ion-Pairing Effects of Choline Acetate Electrolyte in Protic and Aprotic Solvents Studied by NMR Titrations

Emmanouil Veroutis,^{*[a, c]} Steffen Merz,^[a] Rüdiger-A. Eichel,^[a, b] and Josef Granwehr^[a, c]

Choline-based electrolytes have been proposed as environmentally friendly and low-cost alternatives for secondary zinc air batteries. Choline acetate $[\text{Ch}]^+[\text{OAc}]^-$ in protic (D_2O) and aprotic (DMSO-d_6) solvents has been studied by means of concentration-dependent ^1H NMR, viscosity, and density measurements. The viscosities have been calculated on the basis of the Jones-Dole equation and showed that the dominant contribution originates from short-range ion-solvent interactions. Site-specific association affinities were assigned from NMR chemical shift titrations. In DMSO-d_6 , the hydroxyl group of choline was found to have the smallest dissociation constant followed by the methyl group of acetate. The corresponding Gibbs energies at low concentration were found to be in agreement with a solvent-separated ion pair (2SIP) configuration, whereas at concentrations above 300 mM, a solvent-shared ion pair (SIP) configuration was assigned. For $[\text{Ch}]^+[\text{OAc}]^-$ in D_2O , association effects were found to be weaker, attributed to the high dielectric constant of the solvent. On

time scales on the order of 100 ms, NMR linewidth perturbations indicated a change in the local rotational dynamics of the ions, attributed to short-range cation-solvent interactions and not to solvent viscosity. At 184 mM, $\sim 40\%$ of the cations in DMSO-d_6 and $\sim 10\%$ in D_2O were found to exhibit short-range interactions, as indicated by the linewidth perturbations. It was found that at about 300 mM, the ions in DMSO-d_6 exhibit a transition from free to collective translational dynamics on time scales on the order of 400 ms. In DMSO-d_6 , both ions were found to be almost equally solvated, whereas in D_2O solvation of acetate was stronger, as indicated by the obtained effective hydrodynamic radii. For $[\text{Ch}]^+[\text{OAc}]^-$ in DMSO-d_6 , the results suggest a solvent-shared ion association with weak H-bonding interactions for concentrations between 0.3–1 M. Overall, the extent of ion association in solvents such as DMSO is not expected to significantly limit charge transport and hinder the performance of choline-based electrolytes.

1. Introduction

In their traditional form ILs usually incorporate imidazolium and pyridinium moieties which suffer from high toxicity, poor biodegradability, low solubility in aqueous media and high cost.^[1–3] Choline (2-hydroxy-N,N,N-trimethylethan-1-aminium) belongs to a class of water soluble quaternary ammonium salts, $[\text{Ch}]^+[\text{X}]^-$ where X represents the adjustable anion.^[4] Choline, which is abundant in many plants and animal organs as a phospholipid constituent of lecithin, has recently been pro-

posed as an environmentally friendly and low cost alternative for traditional IL cations.^[5–7]

$[\text{Ch}]^+[\text{Cl}]^-$ mixed with either a metal chloride or a hydrogen bond donor such as an amide or a carboxylic acid is used to form a so called “deep eutectic solvent” (DES).^[8–11] The mixture of $[\text{Ch}]^+[\text{Cl}]^-$ and urea at a 1:2 mol ratio exhibits a melting point of 12 °C, which is more than an order of magnitude lower compared to the melting points of the individual constituents. The formation of a DES has been found to depend critically on the formation of H-bonds between the cation and the anion, as well as between the anion and the neutral donor, e.g. an amide or a carboxylic acid.^[12]


Tunable physicochemical characteristics have also been found for mixtures of an IL and a molecular solvent.^[13–16] These characteristics not only depend on the concentration of the species, but also the extent and type of interactions between them. As illustrated by Dupont *et al.*, the pure IL can be considered as a supramolecular complex that forms under the competition of ionic and/or H-bonding interactions.^[17,18] When the IL is diluted, the complex breaks and neutral clusters are formed. At high dilutions, the solution is described as a dilute electrolyte with the existence of contact ion pairs (CIP) or solvent-shared ion pairs (SIP).^[19]


Electrolytes are often referred to as “infinitely” dilute aqueous solutions of simple inorganic salts where the ions are fully dissociated.^[20] In dilute aqueous solutions of monovalent

[a] E. Veroutis, S. Merz, R.-A. Eichel, J. Granwehr
Forschungszentrum Jülich GmbH, Institute of Energy and Climate Research – Fundamental Electrochemistry (IEK-9)
52428 Jülich, Germany
E-mail: e.veroutis@fz-juelich.de

[b] R.-A. Eichel
RWTH Aachen University, Institute of Physical Chemistry, 52062 Aachen, Germany

[c] E. Veroutis, J. Granwehr
RWTH Aachen University, Institute of Technical and Macromolecular Chemistry, 52062 Aachen, Germany

 Supporting information for this article is available on the WWW under <https://doi.org/10.1002/cphc.202100602>

 © 2021 The Authors. ChemPhysChem published by Wiley-VCH GmbH. This is an open access article under the terms of the Creative Commons Attribution Non-Commercial NoDerivs License, which permits use and distribution in any medium, provided the original work is properly cited, the use is non-commercial and no modifications or adaptations are made.

symmetric salts such as NaCl, ion pairs are rarely formed.^[21] As described by Bjerrum,^[22] ion pairing is regulated by the type of solvent; polar/non-polar and the valence of the ions. In particular, it follows from the Debye-Hückel (DH)^[23] theory that the electrostatic interaction between ions tends to be stronger in the presence of a solvent with a low dielectric constant, such as chloroform (CHCl₃) or dichloromethane (DCM).^[24] Bjerrum further considered that ion pairs and free ions in solution will be in thermodynamic equilibrium and hence the law of mass action and an equilibrium association constant could be defined.^[25] This has significant implications since it was then possible to determine the kinetics and the corresponding energies for the ion pairing process.^[26–28]

Since ILs and organic electrolytes tend to exhibit a markedly more diverse interaction landscape than the non-specific electrostatic interactions found in *e.g.* simple metal halide electrolytes, Hunt *et al.* categorized interactions in ILs as H-bonds of three types.^[29] The neutral H-bond X...Y, the ionic H-bond [X]⁺...Y between an ion and a neutral molecule and the double ionic H-bond [X]⁺...[Y]⁻ between two ions. For an IL or IL/solvent mixture these interactions can be operative at the same time.

Ion pairing interactions and solvent competition is another crucial aspect for electrolytes and IL/solvent mixtures,^[30–32] because the extend of ion pairing can potentially limit charge transport and alter the performance of the electrolyte. For example, Robinson and Harned showed that the activities of aqueous solutions of alkali metal halides decrease according to the ionic radius, but for the alkali metal fluorides, hydroxides, formates and acetates the opposite behavior was found.^[33] They rationalized this by a local hydrolysis, whereby an H-bonded solvent-shared ion pair (SIP), [C]⁺...[OH]⁻...[H]⁺...[A]⁻ with the conjugate base acting as an acceptor to the water hydrogen, is formed. This is an ionic H-bond in Hunt's nomenclature.^[29]

Most studies have been concerned with ion pairing on alkylimidazolium ILs. Rogač *et al.* used temperature and concentration dependent conductivity measurements for [C₂C₁Im]⁺ [EtSO₄]⁻ in H₂O, acetonitrile (AN) and DCM.^[34] The obtained association constants showed that ion pairing increases as the permittivity of the solvent decreases. Whereas in H₂O ion pairing was found to be negligible, in AN and DCM association was significant and entropy-driven. Moreover, Katsuta *et al.* showed by conductivity measurements and density functional theory (DFT) calculations for a series of alkyl- and butylimidazolium, as well as tetraalkylammonium ILs in DCM, that not only the solvent, but also the molecular structure of the ions influences the degree of association.^[35]

Studies on ion pairing or hydrogen bonding in choline-based IL/solvent mixtures are not as common.^[36,37] Aqueous solutions of [Ch]⁺[Cl]⁻ and [Ch]⁺[Br]⁻ were described early on by Boyd *et al.* on the basis of electrochemical methods.^[38] It was deduced that the low activity coefficients observed are the result of the hydroxyl group intervening with the H-bonded structure of water. In a more recent study, Willcox *et al.* showed via MD that in choline acetate the hydroxyl group exhibited significant hydrogen bonding with the oxygen atoms of acetate.^[39] Even at 600 K about 67% of cholines still participated

in H-bonding, although only solutes in the gas phase were simulated. Similarly, mixtures of [Ch]⁺[Cl]⁻, urea and DMSO have been studied by Shah *et al.* with MD simulations.^[40] It was found that the number of H-bonds between urea and DMSO became significant at DMSO fractions higher than 70%. The [Ch]⁺...[Cl]⁻ H-bonding interaction occurred directly between –OH and [Cl]⁻ and did not change upon addition of DMSO. This suggests that at fractions below 70% DMSO is not expected to significantly influence the performance of DESs in electrochemical systems.

Spectroscopic techniques such as infrared spectroscopy (IR) or Nuclear Magnetic Resonance (NMR) have been frequently used in the elucidation of ion pairing and solvation phenomena in IL/solvent mixtures.^[41–47] For example, using H/D exchange experiments and Nuclear Overhauser Effect (NOE) NMR, Zanatta *et al.* showed that the preferential deuteration of 1-n-Butyl-2,3-dimethylimidazolium [C₄C₁Im]⁺-type ILs occurs only in aprotic solvents of low dielectric constant such as CHCl₃ or AN.^[48] This was attributed to the existence of a contact ion pair (CIP) rather than on the basicity of the anions. In a combined study by NMR, IR and DFT, Zhang *et al.* showed that [C₄C₁Im]⁺[TFA]⁻ mixed with MeOH and H₂O exhibits significant H-bonding interactions.^[49] The carboxylate of [TFA]⁻ showed preferential association with both solvents at low concentrations, whereas for the [C₄C₁Im]⁺ the solvents associated on the alkyl proton sites.

The electrochemical performance of choline-based electrolytes has been recently assessed by Liu, Sakthivel *et al.* in Zn-air cells.^[50–52] It was found that aqueous choline acetate showed good compatibility with the selected electrode/catalyst and reduction of dendrite formation. It has previously been shown that choline-based ILs exhibit a solvent-shared ion pair (SIP) configuration at high salt concentrations in the presence of H₂O.^[53] Both cation and anion were found to participate in H-bonds with H₂O, but at the same time the high entropic contribution indicated that the organizational structure of H₂O was preserved.

In this study concentration dependent NMR, as well as viscosity and density measurements are used to investigate choline acetate [Ch]⁺[OAc]⁻ in protic water (D₂O) and aprotic dimethyl sulfoxide (DMSO-d₆) solvents. To probe ion-ion/solvent association equilibria, chemical shift titration experiments have been performed. Moreover, by combining diffusion ordered spectroscopy (DOSY) with viscosity measurements the effective hydrodynamic radius of the ions is estimated. Based on these measurements a model for the ion-ion/solvent association in [Ch]⁺[OAc]⁻ is proposed and its behavior between protic and aprotic solvents is outlined.

Experimental Section

Materials and Sample Preparation

Choline acetate salt [Ch]⁺[OAc]⁻ (≥98%, IoLiTec GmbH) was prepared by vacuum drying (*P* ~10⁻⁵ mbar) over night at 90 °C in order to remove absorbed and crystal water. Due to its strong hygroscopic behavior the dried salt was stored in a glovebox under

argon atmosphere (≤ 0.1 ppm H_2O) for further use. The desired molar concentrations (6–796 mM) were obtained by dissolving the dried salt in 2 ml of D_2O ($\sim 99.9\%$ D, Sigma-Aldrich GmbH) and DMSO-d_6 ($\sim 99.9\%$ D, Sigma-Aldrich GmbH). The DMSO samples were prepared inside the glovebox to avoid further contamination of the solvent from moisture. Figure S1 in the SI shows the prepared series of samples for the measurements in this study.

For ^1H chemical shift referencing in the NMR experiments, 1 wt% 3-(trimethylsilyl)-1-propanesulfonic acid sodium salt (DSS) was used in D_2O solutions and 0.03 vol% tetramethylsilane (TMS) in the DMSO-d_6 solutions. The reference standards in the solutions were prepared by Sigma-Aldrich GmbH. Within experimental uncertainty interference from the reference standards on choline acetate solutions was negligible, as deduced from the linewidths and the diffusion coefficients. To quantify the water contamination in DMSO-d_6 a neat sample was additionally measured by NMR (Figure S2). Comparing the signals of H_2O and TMS results in approximately 0.1 vol% H_2O (~ 60 mM). Methanol- d_4 (CD_3OD , $\geq 99.8\%$, Sigma-Aldrich GmbH) was used for calibrating the temperature in the NMR experiments.^[54]

Viscosity and Density Measurements

For the viscosity measurements a TA Instruments AR-G2 rheometer was used with a stainless steel cone plate spindle (\varnothing 60 mm, truncation 0.5°). The temperature of the sample was kept at 23.5°C by a Peltier plate and the sample was allowed to equilibrate for 10 min prior to the measurement. The viscosity was determined by measuring 11 points for shear rates between 100 and 1000 Hz and taking the mean. The data were further processed by linear regression, yielding values within the error ($\pm 2\%$) from the mean.

For the density measurements an Anton Paar DMA 5000 instrument was used with a build-in temperature controller. Temperature was kept at 23.5°C throughout the measurements. The instrument was calibrated using pure water and subsequently with neat D_2O and DMSO-d_6 yielding densities of 1.104 g/cm^3 and 1.185 g/cm^3 , respectively. Before loading each sample, the capillary system of the instrument was rinsed with isopropanol and acetone. Measurement uncertainty was on the order of $\pm 0.001\text{ g/cm}^3$.

NMR Measurements

All NMR experiments were performed using a Bruker Avance III-HD spectrometer operating at 600 MHz ^1H frequency, equipped with a 3-channel H/C/N 5 mm TXI-Z Gradient probe (max. 0.5 T/m at 10 A).

The temperature was regulated with the variable temperature unit (VTU) of the probe by flowing dry nitrogen gas through the sample tube. In all cases temperatures were held constant at $(23.5 \pm 0.3)^\circ\text{C}$ and the sample was allowed to equilibrate for 10 min before each measurement.

All spectra were obtained under quantitative conditions with hard 90° pulses with radio frequency (RF) field strength of $\nu_{\text{RF}} \sim 18\text{ kHz}$ at 10 W, recycle delay of 25 s ($\approx 5T_1$) and 8 accumulations for signal averaging. Spin-lattice relaxation times T_1 were determined using the inversion recovery method^[55] with recovery delays varying from 0.001 s to 40 s in 11 increments.

For the diffusion measurements a pulsed field gradient stimulated echo (PFGSTE) sequence was employed with an additional longitudinal eddy current delay (LED) and two spoil gradients to dephase unwanted transverse magnetization during diffusion and LED periods.^[56] Diffusional mixing Δ and gradient lengths δ were fixed to 200 ms and 1.6 ms for the D_2O solutions and 400 ms and 1.6 ms for the DMSO-d_6 solutions, respectively. The gradient strength g was increased linearly from 0.01 T/m to 0.45 T/m in 16 increments. To obtain the self-diffusion coefficients, the data were fitted using the Stejskal-Tanner relationship.^[57] The experimental uncertainty of the diffusion coefficients was found to be $\pm 3\%$ by repeating the measurement 3 times. Comparing the results to a convection compensated diffusion sequence^[58] it was deduced that convection has no influence on the measurements.

2. Results and Discussion

2.1. Viscosity and Density

Figures 1(a),(b) show the viscosity η and density ρ as a function of $[\text{Ch}]^+[\text{OAc}]^-$ concentration in D_2O and DMSO-d_6 . It is apparent that both viscosity and density show a stronger dependence to concentration in DMSO-d_6 than in D_2O . The

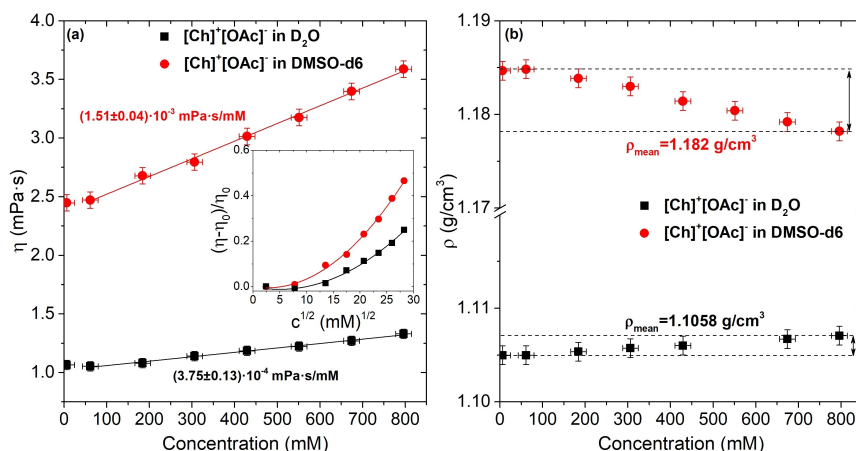


Figure 1. Concentration dependence of viscosity (a) and density (b) for $[\text{Ch}]^+[\text{OAc}]^-$ in D_2O (black) and DMSO-d_6 (red). Solid lines represent linear fits. Inset graph shows the relative viscosity as a function of the square-root of concentration, with the data fitted with Eq. (1). Dashed lines show the range of densities with the mean densities indicated accordingly.

viscosity (Figure 1(a)) is found to increase linearly for both solvents, with a slope of $1.5 \cdot 10^{-3}$ mPa·s/mM in DMSO- d_6 and $3.75 \cdot 10^{-4}$ mPa·s/mM in D $_2$ O.

Calculating the viscosities of electrolytes goes back to the pioneering works by Onsager and Fuoss,^[59] Jones and Dole,^[60] Falkenhagen *et al.*,^[61] and later by Kaminsky^[62] as well as Lencka *et al.*^[63] For electrolytes in the limit of “infinite” dilution the relative viscosity $(\eta - \eta_0)/\eta_0$, where η_0 is the viscosity at highest dilution ($\eta_0^{\text{DMSO-d}_6} = 2.44$ mPa·s, $\eta_0^{\text{D}_2\text{O}} = 1.06$ mPa·s) is linear as a function of the square-root of the concentration. This is valid for electrolytes in the range of 0.1–10 mM. As shown in the inset graph of Figure 1(a) the relative viscosity does not scale linearly with \sqrt{c} for both solvents. For concentrations between 0.1–1 M the deviation from linearity can be described using the approach of Jones and Dole,

$$\frac{\eta - \eta_0}{\eta_0} = A\sqrt{c} + Bc \quad (1)$$

where A accounts for long-range electrostatic interactions in the framework of DH-theory, while B accounts for short range ion-solvent specific interactions. Four contributions have been reported to influence B , (i) ionic solvation *i.e.* the association of the solvent molecules with the ions, (ii) ordering of the solvent molecules by the field of the ions, (iii) structure breaking effects *e.g.* the disruption of the H-bonded structure of water by the inclusion of the ions, and (iv) steric effects.^[62]

The non-linear behavior observed for $[\text{Ch}]^+[\text{OAc}]^-$ indicates that apart from non-specific long range electrostatic interactions, short range association effects in the form of ion-ion or ion-solvent interactions must be operative. Fitting the data with Eq. (1) results in $A = (3.8 \pm 0.7) \cdot 10^{-3} \text{ L}^{1/2} \text{ mmol}^{-1/2}$ and $B = (7.2 \pm 0.3) \cdot 10^{-4} \text{ L/mmole}$ for the DMSO- d_6 solutions and $A = (4.7 \pm 0.6) \cdot 10^{-3} \text{ L}^{1/2} \text{ mmol}^{-1/2}$ and $B = (4.7 \pm 0.3) \cdot 10^{-4} \text{ L/mmole}$ for the D $_2$ O solutions. The larger change observed in DMSO- d_6 should also account for its smaller dielectric constant ($\epsilon_r \sim 47$) as compared to D $_2$ O ($\epsilon_r \sim 78$),^[64] since a solvent with lower permittivity is less effective in shielding local charges. Viscosity is expected to alter the performance of the electrolyte, since

low viscosity allows for leaking of the electrolyte through the porous electrode, whereas high viscosity reduces the contact with the catalyst.

Similar observations were reported by Rodríguez *et al.*^[65] in 1-ethyl-3-methylimidazolium -based H $_2$ O mixtures, where the viscosity was found to increase with decreasing mole fraction of H $_2$ O. Another factor which should be considered is the H-bonded structure of water, which as described by Frank *et al.*,^[66] the inclusion of an ionic solute disrupts the ordering of water molecules. This has found to add a negative contribution to the viscosity of aqueous electrolytes.

For the density (Figure 1(b)) a smaller variation with concentration is observed, as compared to the viscosity. For DMSO- d_6 a variation of 0.006 g/cm^3 with a mean density of 1.18 g/cm^3 is observed, whereas for D $_2$ O the variation is smaller, with 0.002 g/cm^3 and a mean density of 1.1 g/cm^3 . The behavior is also different between the two solvents, where for DMSO- d_6 the density decreases with increasing $[\text{Ch}]^+[\text{OAc}]^-$ concentration, for D $_2$ O it increases, although slightly, with increasing concentration. Similar trend has also been reported for the $[\text{C}_2\text{C}_1\text{Im}]^+ - \text{H}_2\text{O}$ mixtures by Rodríguez *et al.*^[65] and also by Laliberté *et al.*^[67] for MgSO_4 in H $_2$ O.

2.2. NMR Titrations

2.2.1. Chemical-Shift Perturbations

NMR titration experiments offer the possibility to characterize the thermodynamics of association between the ions as well as the ions and the solvent molecules in electrolyte solutions.^[68–71]

^1H chemical shift perturbations (CSPs) are shown in Figure 2 for the functional groups of $[\text{Ch}]^+[\text{OAc}]^-$ in DMSO- d_6 (a) and in D $_2$ O (b), respectively. The perturbations are plotted as $\Delta\delta = \delta_{\text{obs}} - \delta_f$, where δ_{obs} is the shift at each concentration and δ_f is the shift at highest dilution where the molecules are assumed to be free.

In DMSO- d_6 the strongest non-linear CSP is observed for the –OH group of choline, with a maximum deviation of about 0.7 ppm downfield (Figure 2(a)). A downfield shift indicates a

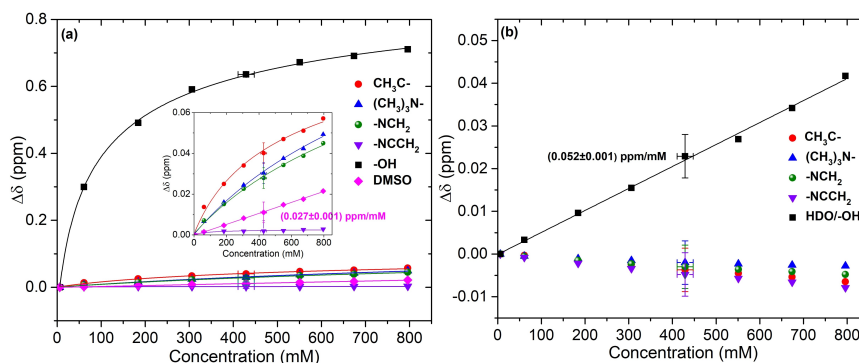


Figure 2. Relative ^1H chemical shifts as a function of $[\text{Ch}]^+[\text{OAc}]^-$ concentration in DMSO- d_6 (a) and D $_2$ O (b). Inset in (a) shows an expansion for the shifts of $\text{CH}_3\text{C}-$, $(\text{CH}_3)_3\text{N}-$, $-\text{NCH}_2$, $-\text{NCCH}_2$ and DMSO. For the shifts of $\text{CH}_3\text{C}-$, $(\text{CH}_3)_3\text{N}-$, $-\text{NCH}_2$, $-\text{NCCH}_2$ and $-\text{OH}$ in (a) solid lines represent fits with Eq. (3), the rest are linear fits.

de-shielding of the donor –OH proton upon removal of electron density due to *e.g.* an H-bond accompanied by an electron density increase on the acceptor site.^[72–74] Downfield chemical shifts have also been observed by Avent *et al.*^[41] for [C₂C₁Im]⁺[Cl,Br,I][–] in AN and attributed to H-bonding interactions between the protons in the imidazolium ring and the anion. Another factor for the shift of the labile –OH proton is the chemical exchange contribution. With increasing [Ch]⁺[OAc][–] concentration, the population of H-bonds with the –OH group increases and the shift moves towards the more populated site (see Eq. (2)). Similar observations were reported for the labile –NH proton of [C₂C₁Im]⁺-type IL with H₂O/D₂O mixtures by Yaghini *et al.*^[15]

For the methyl and methylene groups smaller perturbations were observed. This indicates weaker interactions involving this particular groups. As shown by the inset in Figure 2(a), for the cation and anion protons non-linear downfield shifts with maximum deviations of 0.02–0.06 ppm are observed. The order of perturbation from large to small for the shift is, –OH > CH₃C– > (CH₃)₃N– > –NCH₂ > DMSO > –NCCH₂. The order is also indicative of the electron density variation for the protons in the groups as a result of the intermolecular interactions. The observed shifts are a population weighted average between free and associated states (see section 1.1 in the SI) such that,

$$\delta^{\text{Obs}} = p_f \delta_f + p_a \delta_a \quad (2)$$

where p_f , p_a , δ_f , δ_a , are the fractional populations and shifts of the free and associated molecules respectively. From Eq. (2) and the shifts in Figure 2, the fractional populations p_a for each group can be estimated. The values of p_a at *e.g.* 184 mM are listed in Table 1, with the –OH and CH₃C– of [Ch]⁺ and [OAc][–] showing the largest population respectively. Interactions with the solvent molecules are also indicated by the 0.027 ppm/mM downfield variation observed for the residual non-deuterated methyl groups of DMSO-*d*₆ (DMSO-*d*₃). Since DMSO is a strong base with $\text{p}K_a \approx 35$ ^[75] it can be protonated by a molecule with a similar $\text{p}K_a$. Water in DMSO has been reported to have similar $\text{p}K_a$ as DMSO^[76] and therefore can easily accept a proton from H₂O. At the same time choline can also donate a proton to water, since choline is expected to act as a stronger base in DMSO-*d*₆ than in D₂O. Protonation of acetate, *e.g.* acetic acid $\text{p}K_a \approx 12.3$ in DMSO compared to $\text{p}K_a \approx 4.7$ in H₂O,^[77] from either

water or choline may additionally be a consequence of direct diffusional encounters, rather than a solvent assisted process.

In D₂O the largest perturbation is observed for the shift of HDO/–OH as shown in Figure 1(b). The –OH signal of choline and the residual non-deuterated proton in D₂O (~0.1% HDO) are not separated in the spectrum (Figure S3 in SI) due to fast chemical exchange with the higher fraction of solvent molecules in the sample (see Table S1 in SI). The observed signal is a population weighted average between –OH and HDO which shows a shift perturbation of about 0.04 ppm with a linear downfield variation of 0.052 ppm/mM. The pH and salt dependence on the chemical shift of HDO has been reported to be about $2 \cdot 10^{-3}$ ppm/pH and $9 \cdot 10^{-5}$ ppm/mM respectively upfield.^[78] Therefore, pH and salt variations can be excluded. From Eq. (2) follows that at *e.g.* 184 mM the fractional population p_a of associated HDO is about 24% and increases to about 65% at 550 mM. Within experimental uncertainty no perturbation is observed for the methyl and methylene protons, which indicates that no significant interactions are involved for these groups. This is most likely attributed to the strong ion dissociating character of water.

In order to quantify the thermodynamics of association the CSP isotherms in Figure 2(a) were fitted assuming a 1:1 bimolecular association (see section 1.1 in the SI), by^[69]

$$\delta_{\text{Obs}} = \delta_a + (\delta_f - \delta_a) \left(\frac{-1 + \sqrt{1 + 4K_A \gamma_{\pm}^2 c}}{2K_A \gamma_{\pm}^2 c} \right) \quad (3)$$

where δ_a , δ_f are the shifts at highest and lowest concentration where molecules are assumed to be associated and free respectively, K_A is the association constant, γ_{\pm} is the mean activity coefficient and c the molar concentration. The mean activity coefficients account for the effect of ion electrostatic interaction and are obtained by Eq. (S21), as discussed in sections 1.2 and 2.3 in the SI.

The obtained equilibrium association K_A /dissociation K_D constants with the corresponding Gibbs energy of association ΔG° (Eq. (S3)) are listed in Table 1. As expected from Figure 2 the lowest dissociation constant (highest K_A) is found for the –OH group of choline with $K_D \approx 40$ mM, which corresponds to an association energy of $\Delta G^\circ = -7.5$ kJ/mol. These values are obtained for $\gamma_{\pm} = 0.8$, which corresponds to an ionic strength of $I = 6$ mM. For the other groups except of the methyl group of acetate, larger dissociation constants are found. This indicates that the highest affinity is found for the –OH site and to a lesser degree also for the CH₃– of [OAc][–]. Association constants in the range of 2 M^{-1} were found by Shaukat *et al.* by means of dielectric spectroscopy for aqueous choline chloride solutions.^[79] They assigned the K_A 's to a solvent-shared ion pair (SIP) configuration. From the obtained energies the interactions involving the –OH group are on the limit for weak H-bonds, which is in the range of 8–17 kJ/mol.^[29,72] For the other groups the energies are in the range of van der Waals interactions. This suggests that at low concentration and therefore low ionic strength the majority of ions are in a solvent-separated ion pair (2SIP) configuration.^[19]

Table 1. Equilibrium association K_A , dissociation K_D constants, corresponding energies of association ΔG° and fractional associated populations p_a from the CSP isotherms in Figure 2(a). The association constants shown are obtained with $\gamma_{\pm} = 0.8$ (see sections 1.2 and 2.3 in the SI) and p_a are for 184 mM. For the –NCCH₂ of choline the values could not be obtained due to insignificant shift perturbation, whereas the (CH₃)₂– of DMSO shows a variation which is not described by Eq. (3).

	K_A [M ^{–1}]	K_D [M]	ΔG° [kJ/mol]	p_a [%]
CH ₃ C–	2.36 ± 0.65	0.4 ± 0.1	–2.1 ± 0.7	45
(CH ₃) ₃ N–	0.64 ± 0.15	1.56 ± 0.36	+1.1 ± 0.6	32
–NCH ₂	0.7 ± 0.2	1.4 ± 0.4	+0.9 ± 0.7	40
–NCCH ₂	–	–	–	–
–OH	21.3 ± 1.4	0.04 ± 0.003	–7.5 ± 0.2	70
DMSO	–	–	–	27

Additionally, thermodynamic parameters for different γ_{\pm} values and consequently ionic strength can be found in Table S7 in the SI. At higher ionic strength (or concentration) the dissociation constants were found to decrease. For the –OH group $K_D \approx 12.5$ mM and for the CH_3^- of acetate $K_D \approx 112$ mM was obtained. The energies illustrate this further, for the –OH the association energy increases to $\Delta G^\circ \sim -10.7$ kJ/mol and for the CH_3C^- to $\Delta G^\circ \sim -5.3$ kJ/mol, which suggests an increase in the fraction of ions being in a solvent-shared ion pair (SIP) configuration. For the existence of contact ion pairs (CIP) a higher energy in the range of 17–63 kJ/mol would have been expected.

2.2.2. Linewidth Perturbations

Figure 3(a),(b) shows the linewidth (full width at half maximum FWHM) perturbations for $[\text{Ch}]^+[\text{OAc}]^-$ in DMSO-d_6 and D_2O respectively. Analogous to the CSPs the linewidth perturbations are plotted as $\Delta\Delta\nu_{1/2} = \Delta\nu_{1/2}^{\text{obs}} - \Delta\nu_{1/2}^{\text{f}}$, where $\Delta\nu_{1/2}^{\text{obs}}$ is the linewidth at each concentration and $\Delta\nu_{1/2}^{\text{f}}$ is the linewidth at the highest dilution.

In DMSO-d_6 the strongest perturbation was observed for the –OH group of choline with a maximum deviation of about 80 Hz. The –OH linewidth attains a maximum at about 60 mM, with a subsequent continuous decrease towards higher $[\text{Ch}]^+[\text{OAc}]^-$ concentrations. The concentration at the maximum was also found to coincide with the concentration of H_2O (see Table S1 in the SI) present as impurity in the DMSO-d_6 solutions. Similar to the chemical shifts, the observed linewidths are a population weighted average between free and associated states such that,

$$\Delta\nu_{1/2}^{\text{obs}} = p_f \Delta\nu_{1/2}^{\text{f}} + p_a \Delta\nu_{1/2}^{\text{a}} + \Delta\nu_{1/2}^{\text{ex}} \quad (4)$$

where $\Delta\nu_{1/2}^{\text{f}}$, $\Delta\nu_{1/2}^{\text{a}}$ are the linewidths for the free and associated molecules respectively. The additional contribution $\Delta\nu_{1/2}^{\text{ex}}$ is due to chemical exchange. Chemical exchange broadening contrib-

utes to the observed linewidths due to the difference in proton chemical shifts between the free and associated molecules. Exchange of the –OH proton of choline and H_2O is thermodynamically favorable at ~ 60 mM due to the similar populations, as well as the small difference in pK_a ($pK_a^{\text{Ch}} \approx 13.9$, $pK_a^{\text{H}_2\text{O}} \approx 14$ in water).^[24] Furthermore, the –OH linewidth perturbation must also account for the difference in molecular weights M_W (Eq. (S15) in the SI) since $M_W^{\text{Ch}} > M_W^{\text{H}_2\text{O}}$. At higher concentrations the exchange broadening contribution decreases and the –OH linewidth becomes narrower due to the increase in population of choline relative to water.

Smaller overall perturbations were observed for the methyl groups of choline (CH_3)₃N[–] and of acetate CH_3C^- in both solvents. In DMSO-d_6 a linear deviation was observed for (CH_3)₃N[–] and CH_3C^- with 2.6 mHz/mM and 0.7 mHz/mM, respectively (inset Figure 3(a)). In D_2O a smaller deviation was observed for (CH_3)₃N[–] with 1.6 mHz/mM and a similar deviation of 0.7 mHz/mM for the acetate (Figure 3(b)). The difference in slope between (CH_3)₃N[–] and CH_3C^- is presumably due to the difference in molecular weights since $M_W^{\text{Ch}} > M_W^{\text{OAc}}$ (Table S2 in the SI). As reference, the linewidth of the methyl groups of TMS, the residual non-deuterated methyl groups of DMSO-d_6 (DMSO-d_5) and the methyl groups of DSS are also plotted, and found to show no perturbation.

A similar approach has been followed by Geng *et al.* to evaluate the extent of association in bisquaternary ammonium aqueous electrolytes.^[80] From ⁷⁹Br NMR linewidths they determined K_A 's in the range of 2–13 M^{–1}. From Eq. (4) and the linewidths at lowest and highest concentration the associated fractional population p_a can be obtained. At *e.g.* 184 mM, $p_a \approx 5\%$ for acetate and $p_a \approx 40\%$ and 10% for choline in DMSO-d_6 and D_2O respectively. The obtained p_a 's in D_2O were found to be in good agreement with the fractional coordination obtained by Di Pietro *et al.* for the aqueous choline-based DES system.^[81]

To evaluate the viscosity dependence on the linewidths, $\pi\Delta\nu_{1/2}$ or $\approx R_2$ (Eq. (S9) in the SI) is plotted as a function of viscosity (Figure S5). Similar correlations are observed as in Figure 3, which indicates that the variation of linewidth must

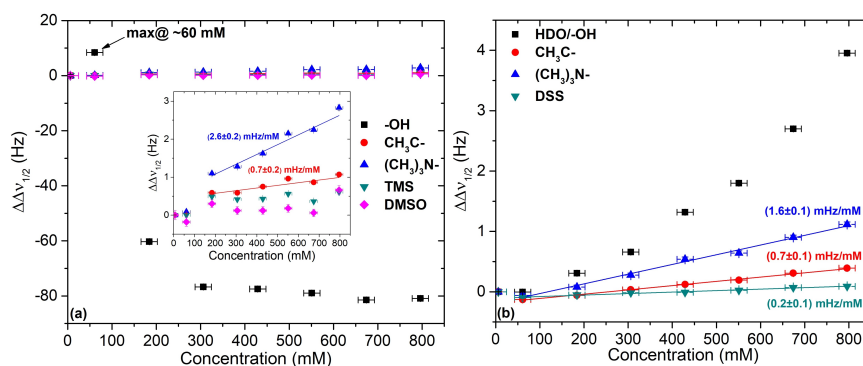


Figure 3. Relative ¹H linewidths (FWHM) as a function of $[\text{Ch}]^+[\text{OAc}]^-$ concentration in DMSO-d_6 (a) and D_2O (b). Inset graph in (a) shows an expansion for the linewidths of CH_3C^- , (CH_3)₃N[–], TMS and DMSO. Solid lines correspond to linear fits.

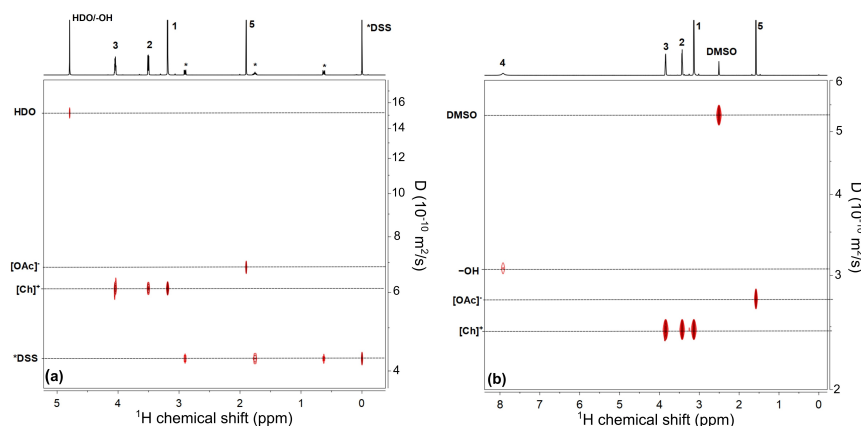


Figure 4. ^1H DOSY spectra for 184 mM $[\text{Ch}]^+[\text{OAc}]^-$ in D_2O (a) and in DMSO-d_6 (b). The different species are separated according to their diffusion coefficients and are indicated by the dashed lines. Due to the small concentration of TMS the DOSY peak is not shown at this contour level.

originate mostly from changes in the local dynamics of the ions and not attributed on the viscosity of the solvents. Considering that the slope of $\text{CH}_3\text{C}-$ of $[\text{OAc}]^-$ is found to be the same in both solvents, the larger slope observed for $(\text{CH}_3)_3\text{N}-$ of $[\text{Ch}]^+$ in DMSO-d_6 suggests stronger cation-solvent interactions for time scales on the order of $T_2 (= 1/R_2)$, *i.e.* ~ 100 ms.

2.3. Diffusion NMR

Diffusion ordered spectroscopy (DOSY) has been often employed in order to assign ionic association and thereby probe correlations in the translational motion of the ions in electrolytes and ILs.^[42,82–84] Figure 4(a),(b) shows the ^1H DOSY spectra for 184 mM $[\text{Ch}]^+[\text{OAc}]^-$ in D_2O and DMSO-d_6 . The components in each mixture are separated due to their difference in the diffusion coefficient. The order from fast to slow diffusion is $\text{HDO} > [\text{OAc}]^- > [\text{Ch}]^+ > \text{DSS}$ for the D_2O and $\text{DMSO} \geq \text{TMS} > -\text{OH} > [\text{OAc}]^- > [\text{Ch}]^+$ for the DMSO-d_6 solutions. The order also reflects the difference in molecular weights (see Table S2 in the SI). In D_2O , the $-\text{OH}$ group of choline cannot be distinguished due to fast exchange with the higher populated HDO, whereas in DMSO-d_6 it is distinguishable and shows a different value compared to $[\text{Ch}]^+$. This is mainly attributed to the exchange of $-\text{OH}$ proton with the H_2O present in the solution. Since the mole fraction of $[\text{Ch}]^+[\text{OAc}]^-$ is higher ($\chi_{\text{ChOAc}} \sim 5.3\%$) than H_2O ($\chi_{\text{H}_2\text{O}} \sim 0.4\%$) at 184 mM (Table S1 in the SI), the diffusion coefficient is weighted more towards choline. Furthermore, from Eq. (5)

$$D^{\text{Obs}} = p_f D_f + p_a D_a \quad (5)$$

follows that the observed diffusion coefficient of HDO at 184 mM corresponds to an associated fractional population p_a of about 20%, whereas for the $-\text{OH}$ in DMSO-d_6 p_a is about 40%.

In Figure 5(a),(b) the diffusion coefficients are shown over the whole concentration range for $[\text{Ch}]^+[\text{OAc}]^-$ in D_2O and

DMSO-d_6 . It is apparent that in both solvents the coefficients show a linear dependence on concentration. In D_2O $[\text{Ch}]^+$, $[\text{OAc}]^-$ and DSS show similar slopes of about $1.5 \cdot 10^{-13} \text{ m}^2/\text{mM}\cdot\text{s}$, while HDO/ $-\text{OH}$ shows a slope of about $2.6 \cdot 10^{-13} \text{ m}^2/\text{mM}\cdot\text{s}$. The difference in the slope can be attributed to the exchange of $-\text{OH}$ and HDO since with increasing concentration the relative populations of choline and HDO change. Similar observations were made for the diffusion of $-\text{OH}$ group in choline-based DES mixtures by D'Agostino *et al.*^[82] The overall decrease in the diffusion coefficient is attributed to the increase in viscosity as shown in Figure 1(a). Plotting the diffusion coefficient as a function of inverse viscosity η^{-1} for $[\text{Ch}]^+[\text{OAc}]^-$ in D_2O (Figure 5(c)) results in linear correlations for both ions, as well as HDO and DSS. For HDO/ $-\text{OH}$ the slope is different (Table 2) which suggests that the viscosity dependence of the solvent molecules is not the same as for the solutes.

As shown in Figure 5(b), in DMSO-d_6 two slopes are observed for $[\text{Ch}]^+$ and $[\text{OAc}]^-$ with a change in slope at about 300 mM. For choline $\sim 1.6 \cdot 10^{-13} \text{ m}^2/\text{mM}\cdot\text{s}$ and $\sim 1.1 \cdot 10^{-13} \text{ m}^2/\text{mM}\cdot\text{s}$ and for acetate $\sim 2.7 \cdot 10^{-13} \text{ m}^2/\text{mM}\cdot\text{s}$ and $\sim 1.3 \cdot 10^{-13} \text{ m}^2/\text{mM}\cdot\text{s}$ are obtained for the low and high concentration range respectively. The change in slope occurs similarly for both ions, which can be attributed to the change from uncorrelated to correlated translational ion mobility. This can be further illustrated by the ratio of cation to anion diffusion coefficients

Table 2. Effective hydrodynamic radii $R_{\text{H}}^{\text{eff}}$ obtained from the slopes in Figure 5(c),(d), a non-solvated molecular radii from Eq. (S12) and b non-solvated radii with the effective density of 0.619 g/cm^3 as suggested by Evans *et al.*, difference between effective hydrodynamic radii and molecular radii $\Delta R = R_{\text{H}}^{\text{eff}} - R^{\text{D}}$.

		slope [$10^{-13} \text{ m}^2 \text{ Pa}$]	$R_{\text{H}}^{\text{eff}}$ [Å]	R [Å] ^a	R [Å] ^b	ΔR [Å]
$[\text{Ch}]^+[\text{OAc}]^-$ in D_2O	$[\text{Ch}]^+$	6.47 ± 0.2	5.08 ± 0.14	2.87	3.5	1.5
	$[\text{OAc}]^-$	6.46 ± 0.2	5.5 ± 0.17	2.38	2.9	2.6
	HDO	9.1 ± 0.5	4.76 ± 0.24	1.66	2.01	2.7
$[\text{Ch}]^+[\text{OAc}]^-$ in DMSO-d_6	$[\text{Ch}]^+$	7.5 ± 0.3	5.55 ± 0.23	2.81	3.5	2.7
	$[\text{OAc}]^-$	9.25 ± 0.6	5.07 ± 0.35	2.32	2.9	2.17
	DMSO	7.2 ± 0.4	6.06 ± 0.4	2.62	3.25	2.8

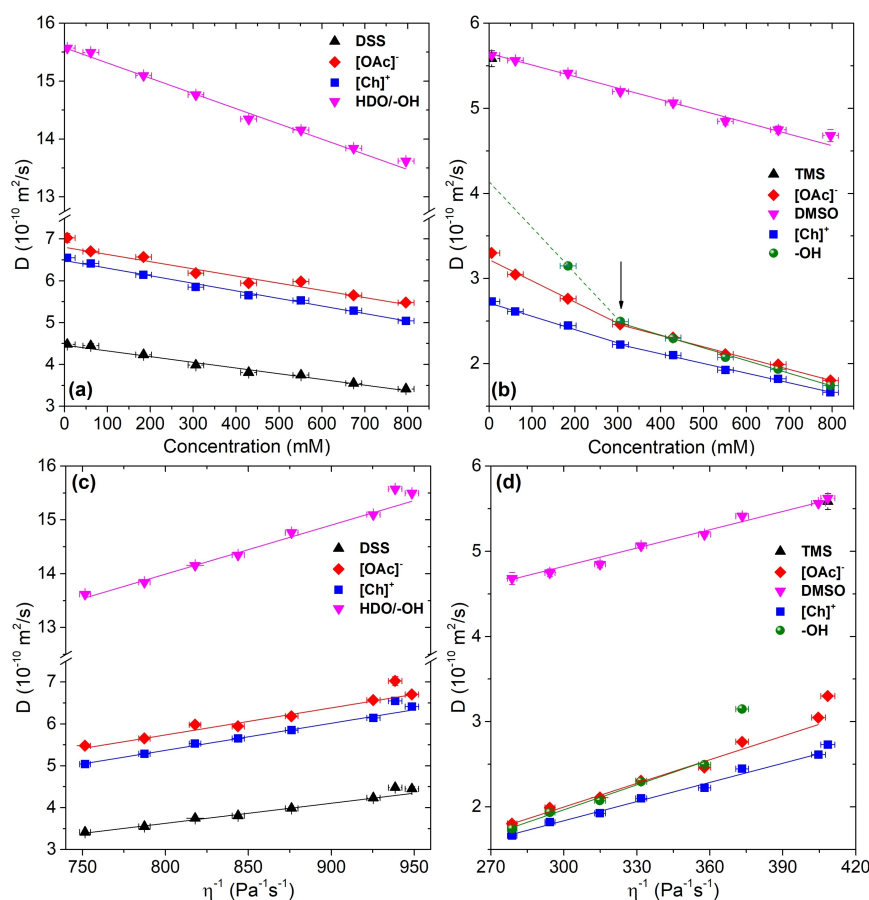


Figure 5. Diffusion coefficients as a function of $[\text{Ch}]^+[\text{OAc}]^-$ concentration in D_2O (a) and in DMSO-d_6 (b) and as a function of inverse viscosity for $[\text{Ch}]^+[\text{OAc}]^-$ in D_2O (c) and in DMSO-d_6 (d). Arrow indicates the concentration at which there is a change in slope. Solid lines correspond to linear fits and the dashed line represents extrapolated data to 6 mM. The diffusion coefficient of TMS has been determined only at the lowest concentration.

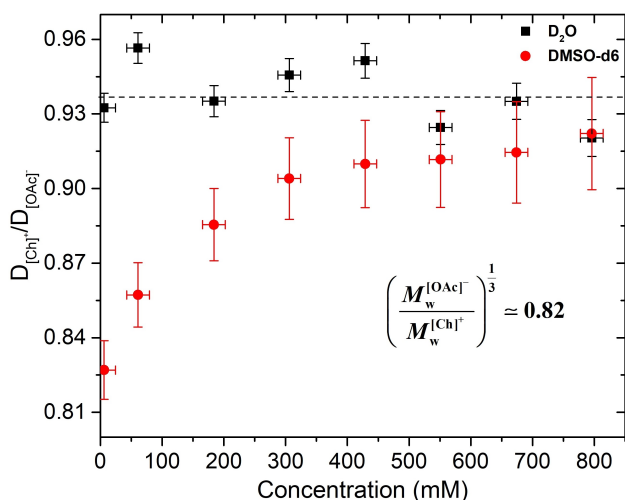


Figure 6. Ratio of cation to anion diffusion coefficients as a function of $[\text{Ch}]^+[\text{OAc}]^-$ concentration in D_2O (black) and DMSO-d_6 (red). Dashed line indicates the mean value of $D_{[\text{Ch}]^+}/D_{[\text{OAc}]^-}$ (~ 0.94) for $[\text{Ch}]^+[\text{OAc}]^-$ in D_2O .

$D_{[\text{Ch}]^+}/D_{[\text{OAc}]^-}$ as shown in Figure 6. Whereas in D_2O no variation is observed, in DMSO-d_6 the ratio increases indicating that the translational mobility of the ions becomes more correlated with increasing concentration. Furthermore, the slope attained for $[\text{Ch}]^+$ beyond 300 mM is similar to the slope of DMSO (Table 2). This indicates that at high concentrations the translational dynamics of cation and solvent are similar, which is also in accordance with the findings from the chemical shift titrations where a solvent-shared ion pair (SIP) configuration was suggested. The diffusion coefficient of the -OH group shows a different slope at low concentrations with $\sim 5 \cdot 10^{-13} \text{ m}^2/\text{mM} \cdot \text{s}$, which is mainly attributed to the exchange of -OH and H_2O . At higher concentrations $D_{-\text{OH}}$ converges to D_{Ch} due to the higher population of choline relative to water.

The ratio of ionic diffusion coefficients can be related to the ratio of molecular weights M_w by the SE equation (Eq. (S19) in the SI),

$$\alpha = \frac{D_{[\text{Ch}]^+}}{D_{[\text{OAc}]^-}} \propto \left(\frac{M_w^{[\text{OAc}]^-}}{M_w^{[\text{Ch}]^+}} \right)^{1/3} \quad (6)$$

The ratio of molecular weights is found to correlate with the ratio of the cation to anion diffusion coefficients α (Figure 6) in DMSO- d_6 indicating low ion association at low concentrations. In D_2O a higher α value is obtained, which cannot be correlated with the ratio of molecular weights. Together with the results from the CSPs this suggests a strong solvation for acetate over the whole concentration range. From the slopes in Figure 5(c),(d) the effective hydrodynamic radii R_H^{eff} of the ions can be obtained using the SE equation. The radii for $[Ch]^+[OAc]^-$ in D_2O and DMSO- d_6 are listed in Table 2 and compared with the non-solvated molecular radii R , as obtained by Eq. (S12) with the experimentally determined densities (Figure 1(b)), as well as with the effective density of 0.619 g/cm^3 as suggested by Evans *et al.*^[85] It has been reported that the SE equation is not valid at high concentrations when *e.g.* ion aggregates or higher order clusters are present.^[86] Nonetheless, the obtained results are used here in a qualitative manner in order to evaluate relative changes in the size of the molecules. From the difference $\Delta R = R_H^{eff} - R$ the size of the solvation layer can be obtained. In D_2O the solvation layer of acetate is about 2.6 \AA , compared to 1.5 \AA for choline, whereas in DMSO- d_6 the layer is larger for choline, with 2.7 \AA as compared to about 2.2 \AA for acetate.^[87,88] A larger solvation layer can potentially hinder the translational motion of the ions, which results in reduced charge transport.

2.4. Association Model

Based on the obtained results, a possible association model for the solutions of $[Ch]^+[OAc]^-$ in DMSO- d_6 and D_2O is suggested. Figure 7 shows four possible associated complexes which are expected to be present at equilibrium. Each functional group is color coded based on the association energies obtained from the chemical shift titrations. Red indicates the highest association affinity while blue the lowest. Complex (AB) corresponds to

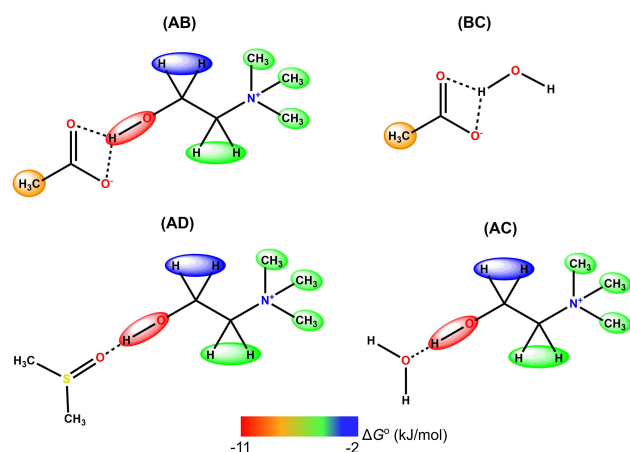


Figure 7. Possible associated complexes formed in the solutions of $[Ch]^+[OAc]^-$ in DMSO- d_6 and D_2O . Color coding corresponds to the association energy ΔG° of each functional group as obtained from the chemical shift titrations for the ionic strength at 796 mM (Table S7 in the SI). Dashed lines indicate H-bonds.

the association of choline and acetate, (BC) of acetate and water, (AC) of choline and water and (AD) of choline and DMSO.

In D_2O the downfield chemical shift and linewidth perturbation observed for the HDO/ $-OH$ resonance indicates that the hydroxyl group of choline is primarily involved, albeit the interaction is not expected to be strong by considering the small shift perturbation and the low mole fraction of $[Ch]^+[OAc]^-$ relative to D_2O . On the diffusion time scale solvation of $[OAc]^-$ was found to be favorable, as indicated by the concentration dependence of the ratio of cation to anion diffusion coefficients, as well as the increase in the effective hydrodynamic radius of acetate. This was also found to be in agreement with the results by Shi *et al.*^[89] where in mixtures of $[C_2C_1Im]^+[OAc]^-$ and water, the acetate anion was shown to be strongly associated with water at high IL dilutions. This points towards a solvent-separated ion pair (2SIP) configuration with equal solvation for $[Ch]^+$ and $[OAc]^-$. A solvent-shared (SIP) or contact-ion pair (CIP) configuration can be excluded for $[Ch]^+[OAc]^-$ in D_2O , which is indicated by the absence of chemical shift perturbation for the methyl and methylene groups and the strong ion dissociating character of water.

In DMSO- d_6 the size of the downfield chemical shift and the linewidth perturbation for the $-OH$ resonance of choline indicates stronger interactions compared to D_2O . Even at low concentrations a $\delta_{-OH} \sim 7\text{--}8 \text{ ppm}$ is suggestive of partial H-bonding interactions with the carboxylate of $[OAc]^-$. For example the $-OH$ proton in neat acetic acid is reported to have a chemical shift of about 11 ppm.^[90] At the same time the maximum observed for the linewidth of $-OH$ at about 60 mM is also found to coincide with the molar concentration of H_2O which is present in the DMSO- d_6 solutions. This suggests that at concentrations between 6–60 mM water competes with $[OAc]^-$ for the interaction with the $-OH$ group. At higher concentrations the relative populations shift towards $[Ch]^+[OAc]^-$ and the interaction with H_2O becomes less favorable. A small downfield shift has also been observed for the resonance of DMSO, indicating solvation and partial association.

Radhi *et al.*^[42] showed by NMR that in mixtures of $[C_2C_1Im]^+[OAc]^-$ and DMSO, the acidic proton in the imidazolium ring preferentially associates with DMSO at low mole fractions ($\chi_{DMSO} < 0.4$), whereas at high mole fractions ($\chi_{DMSO} > 0.6$) DMSO started to associate with the acetate. In their study the concentration and the role of H_2O in DMSO was not discussed. The associated fractional population p_a further suggests that at 184 mM $[Ch]^+[OAc]^-$ in DMSO- d_6 about 70% of $-OH$ is associated. The association energies obtained from the chemical shift perturbations indicate that at high concentrations the interactions involving the $-OH$ group are within the range of weak H-bonds (8–17 kJ/mol), whereas for the methyl and methylene groups they can be assigned to weaker van der Waals -type interactions

On the diffusion time scale, association effects were pronounced at about 300 mM where the translational motion of $[Ch]^+$ and $[OAc]^-$ becomes correlated. At low concentrations the ratio of cation to anion diffusion coefficients coincides with the ratio of molecular weights, which points towards a low ion association at time scales on the order of 400 ms. With

increasing concentration, the ratio of the diffusion coefficients increased, suggesting an increase in ion association although both ions remained solvated, as indicated by the similar effective hydrodynamic radii of DMSO and $[\text{Ch}]^+[\text{OAc}]^-$. The energies and the diffusion coefficients suggest that for $[\text{Ch}]^+[\text{OAc}]^-$ in DMSO- d_6 a solvent-shared ion pair (SIP) configuration is favored for concentrations between 0.3–1 M.

3. Conclusions

The effects of solvation and ion association for $[\text{Ch}]^+[\text{OAc}]^-$ in D_2O and DMSO- d_6 have been elucidated by concentration dependent ^1H NMR, viscosity and density measurements. The dependence on viscosity is modelled by the Jones-Dole equation and is dominated by short-range ion-solvent interactions. In D_2O the NMR CSPs indicate that the $-\text{OH}$ of choline shows preferential proton exchange with HDO, which is attributed to their similarity in $\text{p}K_{\text{a}}$. On the chemical shift time scale for concentrations between 6–800 mM no interaction with the acetate is observed. In DMSO- d_6 the large downfield shift of $-\text{OH}$ indicates partial H-bonding interactions with the acetate even at the lowest concentration. The presence of H_2O as impurity in DMSO facilitates further proton transfer pathways especially at concentrations between 6–60 mM. The solvent is also found to participate in the proton transfer as indicated by the downfield shift of DMSO. It is suggested that the proton transfer equilibrium between $-\text{OH}$ of choline, acetate and H_2O is a result of the smaller $\text{p}K_{\text{a}}$ difference between the species if an aprotic solvent such as DMSO is used. The Gibbs energies obtained from the CSPs in DMSO- d_6 indicate that the interactions involving the $-\text{OH}$ are in the range for weak H-bonds with $\Delta G^\circ \sim -11$ kJ/mol and suggest a solvent-shared ion pair (SIP) configuration for concentrations above 300 mM. On time scales of ~ 100 ms, NMR linewidth perturbations indicate a change in the rotational dynamics of the ions in both solvents although in DMSO- d_6 the change in dynamics of choline is more pronounced. These changes are attributed to local ion-solvent interactions rather than to solvent viscosity. Association effects on time scales of ~ 400 ms are further indicated by PFG-NMR. Above 300 mM both ions and DMSO found to exhibit similar translational dynamics attributed to the solvent-shared ion pair (SIP) configuration. When analyzed using the SE equation, the difference in hydrodynamic radii in D_2O points towards an increase in solvation of acetate although both ions remain equally solvated over the whole concentration range. It is proposed that physicochemical properties such as viscosity and density of $[\text{Ch}]^+[\text{OAc}]^-$ in aprotic solvents with residual H_2O are dominated by short range-ion solvent interactions with solvent shared ion pairs and fast equilibrium proton transfers corresponding to weak H-bonding interactions between the molecules. The extent of short-range interactions for concentrations up to 1 M in solvents such as DMSO is not expected to significantly hinder the performance of choline-based electrolytes. Nonetheless, association effects in analogous solutions need to be taken into consideration for rational design of electrolytes for Zn-air secondary batteries

Acknowledgements

We gratefully acknowledge funding by the German Federal Ministry of Education and Research (BMBF) through project "LuZI" (grant number 03SF0499F). We gratefully acknowledge the Institute of Bioorganic Chemistry (IBOC) at the Forschungszentrum Jülich GmbH and Rainer Goldbaum for providing the 600 MHz spectrometer for the NMR measurements. We gratefully acknowledge Dr. Jörg Stellbrink from Forschungszentrum Jülich GmbH (JCNS-1) for the viscosity and density measurements. Open Access funding enabled and organized by Projekt DEAL.

Conflict of Interest

The authors declare no conflict of interest.

Keywords: choline · acetate · electrolytes · DMSO · NMR

- [1] M. Petkovic, K. R. Seddon, L. P. N. Rebelo, C. S. Pereira, *Chem. Soc. Rev.* **2011**, *40*, 1383–1403.
- [2] A. Romero, A. Santos, J. Tojo, A. Rodríguez, *J. Hazard. Mater.* **2008**, *151*, 268–273.
- [3] T. P. Thuy Pham, C. W. Cho, Y. S. Yun, *Water Res.* **2010**, *44*, 352–372.
- [4] B. L. Gadilohar, G. S. Shankarling, *J. Mol. Liq.* **2017**, *227*, 234–261.
- [5] M. Petkovic, J. L. Ferguson, H. Q. N. Gunaratne, R. Ferreira, M. C. Leitão, K. R. Seddon, L. P. N. Rebelo, C. S. Pereira, *Green Chem.* **2010**, *12*, 643–64.
- [6] Y. Fukaya, Y. Iizuka, K. Sekikawa, H. Ohno, *Green Chem.* **2007**, *9*, 1155.
- [7] P. Nockemann, B. Thijs, K. Driesen, C. R. Janssen, K. Van Hecke, L. Van Meervelt, S. Kossmann, B. Kirchner, K. Binnemans, *J. Phys. Chem. B* **2007**, *111*, 5254–5263.
- [8] A. P. Abbott, R. C. Harris, K. S. Ryder, C. D'Agostino, L. F. Gladden, M. D. Mantle, *Green Chem.* **2011**, *13*, 82–90.
- [9] P. Liu, J.-W. Hao, L.-P. Mo, Z.-H. Zhang, *RSC Adv.* **2015**, *5*, 48675–48704.
- [10] A. P. Abbott, D. Boothby, G. Capper, D. L. Davies, R. K. Rasheed, *J. Am. Chem. Soc.* **2004**, *126*, 9142–9147.
- [11] M. A. R. Martins, S. P. Pinho, J. A. P. Coutinho, *J. Solution Chem.* **2019**, *48*, 962–982.
- [12] C. R. Ashworth, R. P. Matthews, T. Welton, P. A. Hunt, *Phys. Chem. Chem. Phys.* **2016**, *18*, 18145–18160.
- [13] J. Zhao, J. Zhang, T. Zhou, X. Liu, Q. Yuan, A. Zhang, *RSC Adv.* **2016**, *6*, 4397–4409.
- [14] H. Wang, J. Wang, S. Zhang, Y. Pei, K. Zhuo, *ChemPhysChem* **2009**, *10*, 2516–2523.
- [15] N. Yaghini, L. Nordstierna, A. Martinelli, *Phys. Chem. Chem. Phys.* **2014**, *16*, 9266–9275.
- [16] J. D. Holbrey, M. M. Reichert, M. Nieuwenhuyzen, O. Sheppard, C. Hardacre, R. D. Rogers, *Chem. Commun.* **2003**, *3*, 476–477.
- [17] H. K. Stassen, R. Ludwig, A. Wulf, J. Dupont, *Chem. A Eur. J.* **2015**, *21*, 8324–8335.
- [18] J. Dupont, *J. Braz. Chem. Soc.* **2004**, *15*, 341–350.
- [19] Y. Marcus, G. Hefter, *Chem. Rev.* **2006**, *106*, 4585–4621.
- [20] S. Arrhenius, *The Nobel Prize in Chemistry* **1903**, n.d.
- [21] R. M. Fuoss, *Proc. Nat. Acad. Sci.* **1967**, *57*, 1550–1557.
- [22] N. Bjerrum, in *Ergebnisse Der Exakten Naturwissenschaften*, Springer Berlin Heidelberg, Berlin, Heidelberg, **1926**, pp. 125–145.
- [23] E. Hückel, P. Debye, *Phys. Z.* **1923**, *24*, 185–206.
- [24] J. R. Rumble, *CRC Handbook of Chemistry and Physics, 100th Edition*, CRC Press/Taylor & Francis, Boca Raton, FL, **2019**.
- [25] R. M. Fuoss, *J. Am. Chem. Soc.* **1958**, *80*, 5059–5061.
- [26] M. Eigen, K. Tamm, *Zeitschrift für Elektrochemie, Berichte der Bunsengesellschaft für Phys. Chemie* **1962**, *66*, 93–107.
- [27] G. Atkinson, S. K. Kor, *J. Phys. Chem.* **1965**, *69*, 128–133.
- [28] J. Ingenmey, O. Hollóczki, B. Kirchner, in *Encycl. Ion. Liq.*, Springer Singapore, Singapore, **2021**, pp. 1–14.
- [29] P. A. Hunt, C. R. Ashworth, R. P. Matthews, *Chem. Soc. Rev.* **2015**, *44*, 1257–1288.

- [30] C. A. Kraus, *J. Phys. Chem.* **1956**, *60*, 129–141.
- [31] W. R. Gilkerson, *J. Chem. Phys.* **1956**, *25*, 1199–1202.
- [32] J. B. Hyne, *J. Am. Chem. Soc.* **1963**, *85*, 304–306.
- [33] R. A. Robinson, H. S. Harned, *Chem. Rev.* **1941**, *28*, 419–476.
- [34] M. Bešter-Rogač, J. Hunger, A. Stoppa, R. Buchner, *J. Chem. Eng. Data* **2011**, *56*, 1261–1267.
- [35] S. Katsuta, K. Imai, Y. Kudo, Y. Takeda, H. Seki, M. Nakakoshi, *J. Chem. Eng. Data* **2008**, *53*, 1528–1532.
- [36] U. N. Patil, *J. Chem. Sci.* **2020**, *132*, 1.
- [37] J. Restolho, J. L. Mata, B. Saramago, *Fluid Phase Equilib.* **2012**, *322*–323, 142–147.
- [38] G. E. Boyd, A. Schwarz, S. Lindenbaum, *J. Phys. Chem.* **1966**, *70*, 821–825.
- [39] J. A. L. Willcox, H. Kim, H. J. Kim, *Phys. Chem. Chem. Phys.* **2016**, *18*, 14850–14858.
- [40] D. Shah, U. Mansurov, F. S. Mjalli, *Phys. Chem. Chem. Phys.* **2019**, *21*, 17200–17208.
- [41] A. G. Avent, P. A. Chaloner, M. P. Day, K. R. Seddon, T. Welton, *J. Chem. Soc. Dalton Trans.* **1994**, 3405–3413.
- [42] A. Radhi, K. A. Le, M. E. Ries, T. Budtova, *J. Phys. Chem. B* **2015**, *119*, 1633–1640.
- [43] A. D. Headley, N. M. Jackson, *J. Phys. Org. Chem.* **2002**, *15*, 52–55.
- [44] P. Bonhôte, A. P. Dias, N. Papageorgiou, K. Kalyanasundaram, M. Grätzel, *Inorg. Chem.* **1996**, *35*, 1168–1178.
- [45] T. Köddermann, C. Wertz, A. Heintz, R. Ludwig, *ChemPhysChem* **2006**, *7*, 1944–1949.
- [46] Q. G. Zhang, N. N. Wang, Z. W. Yu, *J. Phys. Chem. B* **2010**, *114*, 4747–4754.
- [47] M. N. Garaga, M. Nayeri, A. Martinelli, *J. Mol. Liq.* **2015**, *210*, 169–177.
- [48] M. Zanatta, A.-L. Girard, N. M. Simon, G. Ebeling, H. K. Stassen, P. R. Livotto, F. P. dos Santos, J. Dupont, *Angew. Chem.* **2014**, *126*, 13031–13035; *Angew. Chem. Int. Ed.* **2014**, *53*, 12817–12821.
- [49] Q. G. Zhang, N. N. Wang, S. L. Wang, Z. W. Yu, *J. Phys. Chem. B* **2011**, *115*, 11127–11136.
- [50] Z. Liu, G. Pulletikurthi, F. Endres, *ACS Appl. Mater. Interfaces* **2016**, *8*, 12158–12164.
- [51] Z. Liu, G. Li, T. Cui, A. Borodin, C. Kuhl, F. Endres, *J. Solid State Electrochem.* **2018**, *22*, 91–101.
- [52] M. Sakthivel, S. P. Batchu, A. A. Shah, K. Kim, W. Peters, J. F. Drillet, *Materials (Basel)*. **2020**, *13*, 1–21.
- [53] E. Veroutis, S. Merz, R. A. Eichel, J. Granwehr, *J. Mol. Liq.* **2021**, *322*, 114934.
- [54] R. E. Hoffman, *Magn. Reson. Chem.* **2006**, *44*, 606–616.
- [55] A. Abragam, *The Principles of Nuclear Magnetism*, Oxford University Press, **1961**.
- [56] A. S. Altieri, R. A. Byrd, D. P. Hinton, *J. Am. Chem. Soc.* **1995**, *117*, 7566–7567.
- [57] E. O. Stejskal, J. E. Tanner, *J. Chem. Phys.* **1965**, *42*, 288.
- [58] A. Jerschow, N. Müller, *J. Magn. Reson.* **1997**, *125*, 372–375.
- [59] L. Onsager, R. M. Fuoss, *J. Phys. Chem.* **1932**, *36*, 2689–2778.
- [60] G. Jones, M. Dole, *J. Am. Chem. Soc.* **1929**, *51*, 2950–2964.
- [61] H. Falkenhagen, E. L. Vernon, *London, Edinburgh, Dublin Philos. Mag. J. Sci.* **1932**, *14*, 537–565.
- [62] M. Kaminsky, *Discuss. Faraday Soc.* **1957**, *24*, 171–179.
- [63] M. M. Lencka, A. Anderko, S. J. Sanders, R. D. Young, *Int. J. Thermophys.* **1998**, *19*, 367–378.
- [64] J. K. Guillory, *J. Med. Chem.* **2007**, *50*, 590–590.
- [65] H. Rodríguez, J. F. Brennecke, *J. Chem. Eng. Data* **2006**, *51*, 2145–2155.
- [66] H. S. Frank, M. W. Evans, *J. Chem. Phys.* **1945**, *13*, 507–532.
- [67] M. Laliberté, W. E. Cooper, *J. Chem. Eng. Data* **2004**, *49*, 1141–1151.
- [68] P. Bonhôte, A.-P. Dias, N. Papageorgiou, K. Kalyanasundaram, M. Grätzel, *Inorg. Chem.* **1996**, *35*, 1168–1178.
- [69] W. J. DeWitte, L. Liu, E. Mei, J. L. Dye, A. I. Popov, *J. Solution Chem.* **1977**, *6*, 337–348.
- [70] F. Aradi, A. Földesi, *Magn. Reson. Chem.* **1985**, *23*, 375–378.
- [71] A. D. Pauric, S. Jin, T. J. Fuller, M. P. Balogh, I. C. Halalay, G. R. Goward, *J. Phys. Chem. C* **2016**, *120*, 3677–3683.
- [72] S. Scheiner, *Molecules* **2016**, *21*, 1426.
- [73] H. M. Lee, N. J. Singh, K. S. Kim, *Hydrogen Bonding – New Insights*, Springer Netherlands, **2006**.
- [74] G. Gilli, P. Gilli, *The Nature of the Hydrogen Bond*, Oxford University Press, **2009**.
- [75] C. Lee, H. Son, S. Park, *Phys. Chem. Chem. Phys.* **2015**, *17*, 17557–17561.
- [76] I. M. Kolthoff, T. B. Reddy, *Inorg. Chem.* **1962**, *1*, 189–194.
- [77] F. G. Bordwell, *Acc. Chem. Res.* **1988**, *21*, 456–463.
- [78] D. S. Wishart, C. G. Bigam, J. Yao, F. Abildgaard, H. J. Dyson, E. Oldfield, J. L. Markley, B. D. Sykes, *J. Biomol. NMR* **1995**, *6*, 135–140.
- [79] S. Shaukat, M. V. Fedotova, S. E. Kruchinin, M. Bešter-Rogač, Č. Podlipnik, R. Buchner, *Phys. Chem. Chem. Phys.* **2019**, *21*, 10970–10980.
- [80] Y. Geng, L. S. Romsted, *J. Phys. Chem. B* **2005**, *109*, 23629–23637.
- [81] M. E. Di Pietro, O. Hammond, A. Van Den Bruinhorst, A. Mannu, A. Padua, A. Mele, M. Costa Gomes, *Phys. Chem. Chem. Phys.* **2021**, *23*, 107–111.
- [82] C. D'Agostino, L. F. Gladden, M. D. Mantle, A. P. Abbott, E. I. Ahmed, A. Y. M. Al-Murshedi, R. C. Harris, *Phys. Chem. Chem. Phys.* **2015**, *17*, 15297–15304.
- [83] S. A. Krachkovskiy, J. D. Bazak, S. Fraser, I. C. Halalay, G. R. Goward, *J. Electrochem. Soc.* **2017**, *164*, A912–A916.
- [84] G. L. Burrell, I. M. Bargar, Q. Gong, N. F. Dunlop, F. Separovic, *J. Phys. Chem. B* **2010**, *114*, 11436–11443.
- [85] R. Evans, Z. Deng, A. K. Rogerson, A. S. McLachlan, J. J. Richards, M. Nilsson, G. A. Morris, *Angew. Chem. Int. Ed.* **2013**, *52*, 3199–3202; *Angew. Chem.* **2013**, *125*, 3281–3284.
- [86] T. Köddermann, R. Ludwig, D. Paschek, *ChemPhysChem* **2008**, *9*, 1851–1858.
- [87] S. Kerisit, M. Vijayakumar, K. S. Han, K. T. Mueller, *J. Chem. Phys.* **2015**, *142*, 22.
- [88] N. N. Rajput, T. J. Seguin, B. M. Wood, X. Qu, K. A. Persson, *Elucidating Solvation Structures for Rational Design of Multivalent Electrolytes – A Review*, Springer International Publishing, **2018**.
- [89] W. Shi, K. Damodaran, H. B. Nulwala, D. R. Luebke, *Phys. Chem. Chem. Phys.* **2012**, *14*, 15897.
- [90] D. P. Birnie, N. J. Bendzko, *Mater. Chem. Phys.* **1999**, *59*, 26–35.

Manuscript received: August 15, 2021

Revised manuscript received: October 22, 2021

Accepted manuscript online: October 28, 2021

Version of record online: November 3, 2021